

Technical Note

# Design of a novel non-equilibrium plasma-based water treatment reactor

Yanzong Zhang<sup>\*</sup>, Jingtang Zheng, Xianfeng Qu, Honggang Chen

State Key Laboratory of Heavy Oil Processing, China University of Petroleum, Dongying 257061, Shandong, P.R. China

Received 3 April 2007; received in revised form 5 September 2007; accepted 6 September 2007

Available online 29 October 2007

## Abstract

A novel non-equilibrium plasma-based water treatment reactor consisting of high voltage multi-needle electrode submerged in aqueous phase and reticulated ground electrode suspended in gas phase above water was developed and applied to treat low concentrations of methyl orange (MO). The electrode configuration was optimized. Higher number and more uniform distribution of streamers were produced in gas phase when parallel five-needle configuration with needle spacing of 10 mm for high voltage electrode, macroporous ground electrode with mesh size of 0.42 mm, and electrode gap of 17 mm were adopted. This case corresponds to the largest amount of hydrogen peroxide and ozone produced in aqueous phase and gas phase, respectively, and air flow rate presents an economical value. The injection of wastewater above ground electrode for pretreatment and the design of fixed mesh barriers further increase the amount of ozone dissolved in aqueous solution. The conversion of MO presents a positive correlation with input voltage and the increase of pulse repetition rate is conducive for the conversion. In addition, the effect of initial solution concentration and treating volume on the conversion, energy yield and COD removal was evaluated.

© 2007 Elsevier Ltd. All rights reserved.

**Keywords:** Pulse discharge; Hydrogen peroxide; Ozone; Conversion; Energy yield; COD removal

## 1. Introduction

In recent years, the technology of water treatment by non-equilibrium plasma has been attracting more and more attention (Locke et al., 2006). The technology mainly works to oxidize and decompose organic pollutants in water by chemical active species generated from high voltage pulsed discharge. It can completely mineralize organic pollutants with almost no secondary pollution (Mok et al., 2003). For liquid phase high voltage pulsed discharge, oxygen (air) is introduced through hollow needle electrode. The  $\cdot\text{OH}$ ,  $\text{O}^{\cdot}$ ,  $\text{HO}_2^{\cdot}$ ,  $\text{H}_2\text{O}_2$ ,  $\text{O}_3$ , and other active species generated by discharge are utilized to degrade organic pollutants (Kirkpatrick and Locke, 2005; Vel Leitner et al.,

2005; Wang et al., 2006; Hao et al., 2007). The introduction of gas improves the discharge effect, increases plasma channel volume and the quantity of active species. However, because of the difference in relative dielectric constant of water and gas, which is 80 and 1, respectively, high voltage is difficult to be applied to the mixed medium. With the introduction of oxygen, more ozone can be produced, while the generation of hydrogen peroxide is inhibited (Grymonpré et al., 2003). For gas phase high voltage pulsed discharge, ozone is produced in gas phase, and then it diffuses into water and reacts with pollutants (Grabowski et al., 2006, 2007). This kind of reactor features simple design and high space efficiency (corona covers almost the whole space). The combination of liquid phase and gas phase discharge process has been investigated and synergistic effect has been observed in the combined treatment (Yang et al., 2005). Gas–liquid series or parallel discharge reactor possesses the advantages of both liquid and gas

<sup>\*</sup> Corresponding author. Tel.: +86 546 8395397; fax: +86 546 8395190.  
E-mail address: [zh.plasma@yahoo.com.cn](mailto:zh.plasma@yahoo.com.cn) (Y. Zhang).

phase discharge, in which the active species generated in liquid and gas phase cooperate to treat the organic wastewater, and increase the decomposition efficiency of organic pollutants (Grymonpré et al., 2004; Lukes et al., 2004, 2005; Zhang et al., 2007). But only part of ozone dissolved in water is used, and the energy yield is low.

In this paper, a novel non-equilibrium plasma-based water treatment reactor was designed and methyl orange (MO) was used as a model pollutant. The factors that may impact the plasma reaction, including electrode structure, electrode gap, input voltage, pulse repetition rate and air flow rate, were investigated.

## 2. Experimental apparatus and method

The experimental apparatus is made up of a pulse power supply and a non-equilibrium plasma-based water treatment reactor. Voltage and pulse repetition rate range of the pulse power supply (DMG-60) is 0–60 kV and 0–320 pulses per second (pps), respectively. Output capacitance is 67 pF and pulse rise time is less than 100 ns. The reactor, as illustrated in Fig. 1, is a Plexiglas cylinder (inner diameter 35 mm and height 400 mm) with cooling water jacket for temperature control. It mainly consists of high voltage electrode, ground electrode, stainless steel mesh barrier, circulation tube, peristaltic pump (ATP-3200) and sampling pipe. Compressed air is pumped into the air chamber through a gas flow-meter and air inlet tube, and then it passes through the ground electrode and enters the discharge region. The power supply applies voltage to the high voltage electrode submerged in liquid phase and the ground electrode suspended in gas phase, thus electric discharge forms in the aqueous phase along gas–liquid interface and the gas phase above solution interface. Active species such as hydroxyl radicals and hydrogen peroxide are produced in the liquid phase, while ozone is generated

in the gas phase (Lukes et al., 2004, 2005). Hydroxyl radicals, hydrogen peroxide, and ozone diffused in water react directly with MO in the liquid phase, which is called the main oxidation zone. Meanwhile, wastewater is injected above the ground electrode and ozone, as it rises, reacts with MO in solution; in this way, a pre-oxidation zone is formed. Circulation tube and peristaltic pump realize the circulation of solution in the pre-oxidation and main oxidation zone. The synergistic combination of both gas and liquid discharge occurs through peroxone process between ozone dissolved in water and hydrogen peroxide produced in the liquid phase, which brings in additional formation of hydroxyl radicals (Lukes and Locke, 2005). The flow rate of circulating pump and circulation tube is  $0.11 \text{ min}^{-1}$ , which can keep the solution level unchanged in the main oxidation zone and maintain stable discharge.

Hypodermic needles and acupuncture needles are manufactured with stainless steel containing 18–20% of chromium, 8–11% of nickel and 2% of molybdenum. The concentration of MO was monitored during experiments by UV–vis absorption spectroscopy (UV-762). The MO quantity was characterized by absorption peak at 465 nm. The conductivity and pH of the initial and treated solution was measured by conductivity meter (DDS-11A) and pH meter (pHSJ-3F), respectively. The solution concentration used was  $40 \text{ mg l}^{-1}$  with pH of 6.10 and conductivity of  $15 \text{ }\mu\text{S cm}^{-1}$ . The cleaning process was characterized by two parameters. They were defined as (Grabowski et al., 2007):

$$\text{Conversion (\%)} = 100 \times \frac{\text{actual concentration}}{\text{initial concentration}} \quad (1)$$

$$\text{Energy yield [g (kWh)}^{-1}\text{]} = \frac{\text{amount of MO converted (g)}}{\text{energy spent (kWh)}} \quad (2)$$

COD was measured with CM-02 COD analyzer based on the method of acidic oxidation by dichromate (Qu et al., 2007). The pulsed input voltage and current were measured using digital oscilloscope (TDS 1012) with high voltage probe (Tektronix P6015A) and current transducer (HIOKI 3274). The input power from power supply to the reactor was calculated using the following equation (Malik et al., 2002):

$$P = \frac{1}{2} CfU^2 \quad (3)$$

where  $C$  is storage capacitance,  $f$  is pulse repetition rate and  $U$  is input voltage. Energy loss in the reaction system was ignored and the input energy was considered as the total energy acting to convert MO in water. The average power dissipated in the reactor was 7.1 W when input voltage was 46 kV and pulse repetition rate was 100 pps, i.e. the energy per pulse supplied into the reactor was 71 mJ in all experiments presented. The concentration of dissolved ozone was determined by the Indigo method (Bader and Hoigne, 1981). The concentration of hydrogen peroxide was determined by the colorimetric titration (Selles, 1980). All

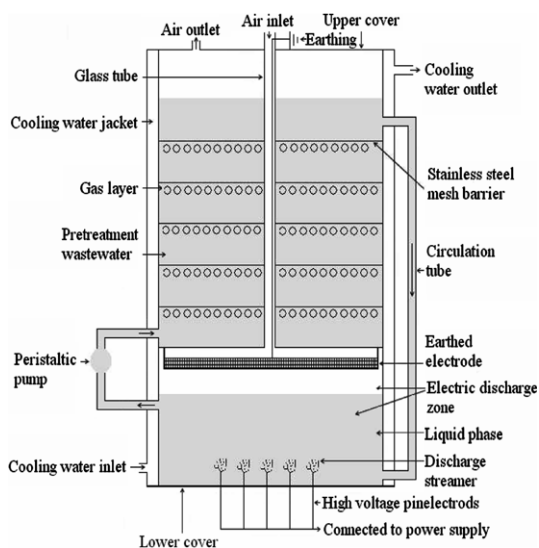


Fig. 1. Detailed schematic of non-equilibrium plasma-based water treatment reactor.

experiments were conducted in triplicate and gave reproducibility of within 5%.

### 3. Results and discussion

#### 3.1. Effect of high voltage electrode configuration

The high voltage electrode was fabricated using acupuncture needle or hypodermic needles with different diameter, and was introduced into the reactor through a rubber plug at the bottom of the reactor and protruded 4 mm. It was submerged in aqueous solution for a distance of 12 mm from liquid surface. The ground electrode was positioned 5 mm above solution in gas phase, that is, the electrode gap was 17 mm. The input voltage was 46 kV with 100 pps and the air flow rate was  $48 \text{ l h}^{-1}$ . Fig. 2a indicates that the conversion increased with the decrease of electrode diameter. After 15 min of discharge, the conversion was the highest for acupuncture needle. To generate electric discharge in water, a highly localized electric field is needed. In practice this can be realized by applying high voltage pulses to sharp electrode that can produce a highly non-uniform electric field in the local region surrounding the electrode tip (Locke et al., 2006). In this way, the emitted electrons can be accelerated to higher energy and more active species can be produced from the collision between electrons and water or oxygen molecules.

The high voltage electrode with two acupuncture needles in parallel was tested. Fig. 2b shows that a certain range of

maximal conversion existed along with the change of needle spacing. The reason may be that the electric field generated around a needle was influenced by neighboring needles in discharge. The highest electric field intensity is generated in the vicinity of needle tip and it decreases with the increase of spatial distance. Moreover, electron kinetic energy is exclusively determined by the local electric field and it increases with the increase of electric field strength (Chen and Davidson, 2002). When needle spacing was 12 mm, there was no superposition of electric fields between two needles and such case corresponds to least amount of energetic electrons. At an appropriate needle spacing (6 mm), the electric field produced by two needles could be strengthened each other by partial superposition and it was conducive to the transfer of energetic electrons (Li et al., 2007). The electric fields between two needles would superpose to a large extent when needle spacing was 4 mm or less, and the electric field intensity around needles would be reduced (Kim and Hong, 2002), thus leading to less energetic electrons. As a result, when needle spacing is 12, 6 and 4 mm, the concentration of dissolved ozone and hydrogen peroxide in water is 0.002, 0.005, 0.003 mM (for ozone) and 0.64, 0.78, 0.7 mM (for hydrogen peroxide), respectively. The voltage and current waveforms corresponding to needle spacing of 6 mm are presented in Fig. 2c. The peak voltage was about 46 kV with pulse rise time of 23 ns and duration of approximately 46 ns. The maximum current was 2.6 A with duration of approximately 50 ns.

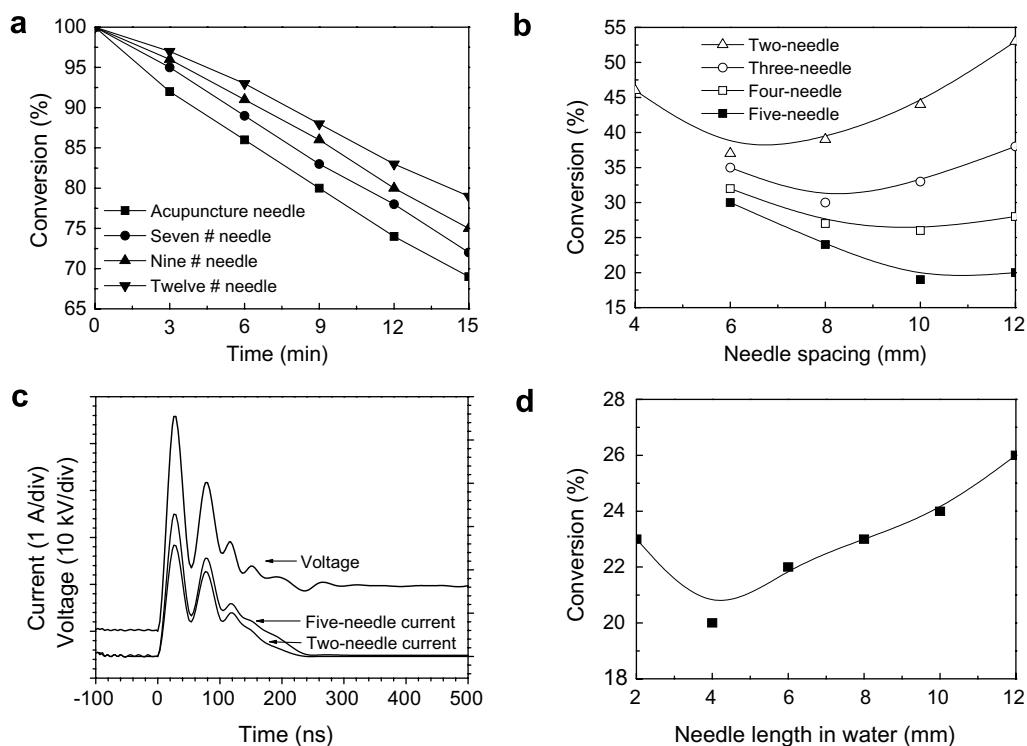


Fig. 2. Effect of electrode diameter (a), needle spacing (b) and needle length in water (d) on conversion and multi-needle configuration on voltage and current waveforms (c) (conditions: ground electrode with mesh size of 0.42 mm; electrode gap 17 mm; input voltage 46 kV with 100 pps; air flow rate  $48 \text{ l h}^{-1}$ ; solution concentration  $40 \text{ mg l}^{-1}$ ; treating volume 0.1 l; discharge 15 min).

Further, three to five needles in parallel with needle spacing of 6, 8, 10 and 12 mm were studied, respectively. As shown in Fig. 2b, for three-needle configuration, the highest conversion occurred at needle spacing of 8 mm (at this time, ozone: 0.007 mM; hydrogen peroxide: 0.84 mM); the highest conversion presented at 10 mm for four-needle cases (ozone: 0.008 mM; hydrogen peroxide: 0.88 mM). For five-needle case with needle spacing of 10 mm, the uniformity of electric field on the concurrent plane of the needles was enhanced, resulting in the increase of stability of electric discharge. Consequently, more streamers were produced, which homogeneously filled almost the whole space between water surface and ground electrode, then more active species were generated (ozone: 0.011 mM; hydrogen peroxide: 0.94 mM), and the conversion represents the highest. The current waveform of this configuration is also presented in Fig. 2c. As for various needle numbers, although the voltage waveform did not change, the current waveform was largely influenced. Current increased and current rise time became shorter with the increase of needle numbers. In five-needle case, current developed synchronistically with the variation of voltage.

The length of needle electrodes protruding from rubber plug into water, which may affect the conversion, was also investigated and the results are shown in Fig. 2d. The conversion increased first and then decreased with the increase of the length, and the highest value occurred at length of 4 mm. This may be explained by that the electric discharge

also occurred below needle tip because of the small curvature radius of acupuncture needles (diameter 0.25 mm), which could increase electron density near the wire. While for a large length, partial electric field below the needle tip was weakened, resulting in decreased number of energetic electrons. Thus the active species produced in pulse discharge was decreased and the conversion was reduced.

### 3.2. Effect of electrode gap, air flow rate and mesh size of ground electrode

To change electrode gap, the distance between high voltage electrode and liquid surface was maintained at 12 mm while the gas layer height between ground electrode and liquid surface was changed to 3, 5, 7, 9 and 11 mm, respectively. As shown in Fig. 3a, with the increase of electrode gap, the conversion increased first and then decreased. The electric field between electrodes depends mainly on the distance between them when input voltage keeps unchanged. With a large electrode gaps (23 mm), the small discharge current was formed because of the weakened electric field, then few and bright streamers and less active species (ozone: 0.005 mM; hydrogen peroxide: 0.78 mM) were produced, so the conversion was low. More streamers were available with the decrease of discharge gap. At electrode gap 17 mm, the mentioned regime was characterized by more streamers distributed bush like and also by relatively larger discharge currents. As a result, the highest conversion was obtained (ozone: 0.011 mM; hydrogen per-

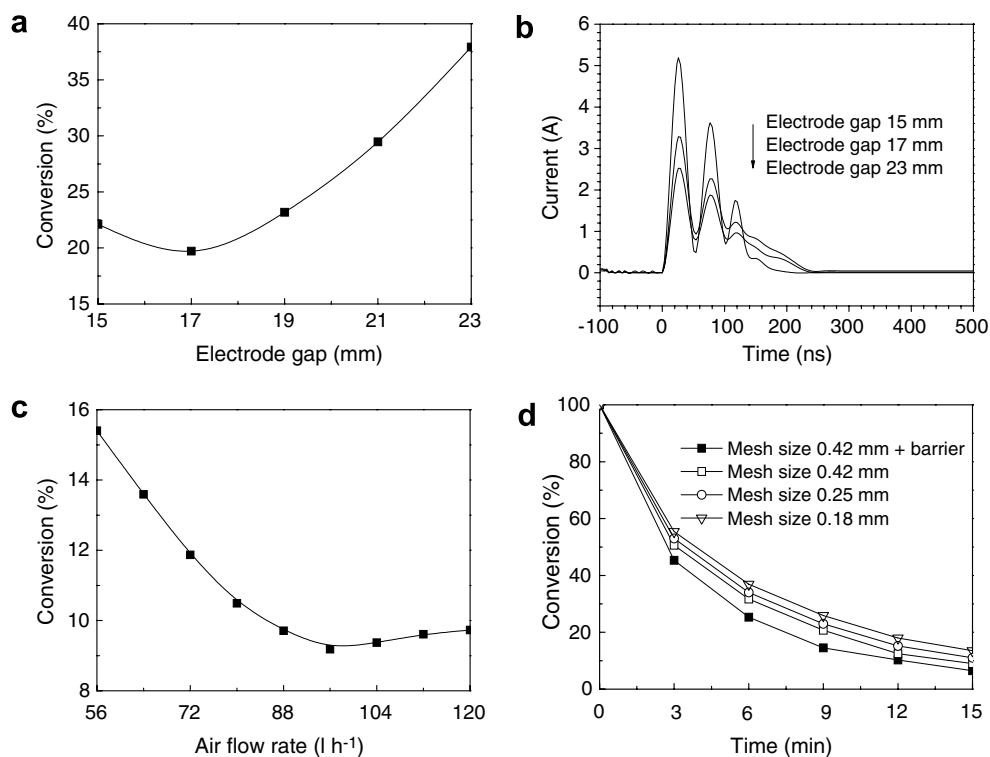


Fig. 3. Effect of electrode gap (a), air flow rate (c) and mesh size of ground electrode (d) on conversion and electrode gap on current waveforms (b) (conditions: five-needle in parallel with needle spacing of 10 mm; needle length in water 4 mm; input voltage 46 kV with 100 pps; solution concentration 40 mg l<sup>-1</sup>; treating volume 0.1 l; discharge 15 min).

oxide: 0.94 mM). For lesser electrode gap 15 mm, the spark discharge could occur on several needle points. In the case of spark discharge, several plasma channels were formed between high voltage electrode and ground electrode, but the channel has a high peak current compared with the streamer discharge (Yao et al., 2001). The increase of current implies higher energy input into the reactor, but compared with streamer discharge, the dissolved ozone concentration was reduced from 0.011 to 0.009 mM and the concentration of hydrogen peroxide in water had essentially no change. It is well known that the temperature in plasma channel during spark discharge is very high, which may result in decomposing of ozone. Fig. 3b shows the current waveforms of various electrode gaps configurations. The current increased with decrease of electrode gaps, and as the gap decreased to 3 mm (spark discharge), the discharge current increased hugely.

Erosion of needle electrodes by pulsed corona discharge in water has been investigated by other researchers from the viewpoint of electrode material and solution conductivity (Lukes et al., 2006). The erosion of needle electrodes was also investigated under the experimental conditions used in this work. For electrode gap of 17 mm (streamer discharge), the mass loss of needle electrodes was negligible and the two-needle electrode became more fragile after operating for 20 h, whereas five-needle electrode only became fragile after 100 h. For electrode gap of 15 mm (spark discharge), much pronounced effect was observed. The mass loss was close to one fourth for five-needle electrode after operating for 2 h, however, the mass loss even reached one half after 2 h for two-needle electrode. So, to keep stable discharge, the electrode gap of 17 mm was chosen in the present study.

Fig. 3c indicates that the conversion improved with the increase of air flow rate. The highest conversion was obtained when air flow rate was  $96 \text{ l h}^{-1}$  (ozone: 0.016 mM; hydrogen peroxide: 0.94 mM). The reaction between ozone and organic solutions belongs to gas–liquid interfacial reaction. Under usual conditions, the transfer of ozone from gas phase to liquid phase pertains to liquid film control process, thus, the increase of air flow rate is helpful

to such transfer. However with the further increase of air flow, the residence time of ozone in pre-oxidation zone is shortened, accordingly, the utilization efficiency of ozone is decreased.

As shown in Fig. 3d, the conversion increased with the increase of mesh size of ground electrode. Macroporous electrode allows the flow of solution through ground electrode thus the degree of mixing in the reactor is increased. In addition, the gas evolved in the discharge can easily pass through porous electrode (Grymonpré et al., 2004). The weak streamer produced between water surface and ground electrode in discharge moved from place to place when the ground electrode with mesh size of 0.18 mm was used. Similar phenomenon took place on the ground electrode with mesh size of 0.25 mm. Whereas for the ground electrode with mesh size of 0.42 mm, the streamers produced were more and tended to stay at a place, and the intensity was higher.

Stainless steel mesh barriers were fixed in pre-oxidation zone and gas layers were formed below the barriers, which retarded the rise of ozone and prolonged the residence time of ozone in pretreated wastewater. For this reason, the dissolved ozone concentration in pretreated wastewater was increased from 0.016 to 0.022 mM compared with the case of no barriers. The introduction of barriers allows sufficient reaction between ozone and MO. On the other hand, liquid film was formed on the barriers, which increased the contact area between ozone and MO, thus the reaction was expedited. The corresponding experimental results are also shown in Fig. 3d. The too large or small distance between two barriers might cause the fluctuation of gas layer and liquid volume between them, which is unfavorable for the mass transfer of ozone and the proceeding of oxidation reactions. In our reactor, the distance between two barriers is configured to be 30 mm and total of six barriers are designed.

### 3.3. Effect of input voltage and pulse repetition rate

As indicated in Fig. 4a, the conversion increased with the increase of input voltage. This is because that at higher

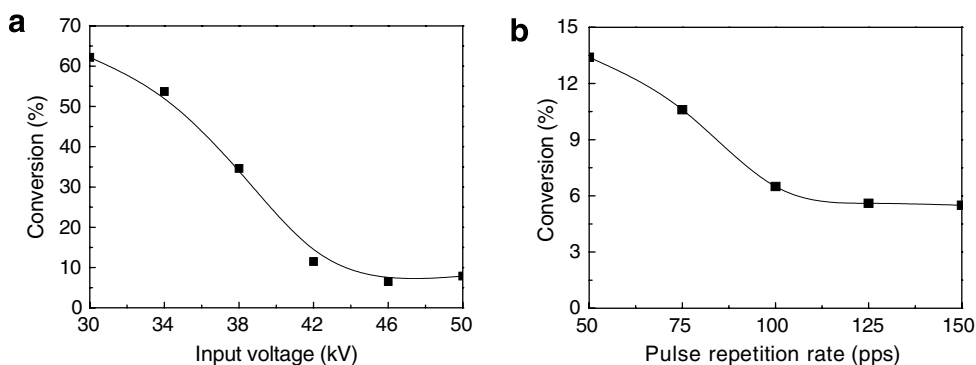


Fig. 4. Effect of input voltage and pulse repetition rate on conversion (conditions: five-needle in parallel with needle spacing of 10 mm; needle length in water 4 mm; ground electrode with mesh size of 0.42 mm; electrode gap 17 mm; air flow rate  $96 \text{ l h}^{-1}$ ; solution concentration  $40 \text{ mg l}^{-1}$ ; treating volume 0.1 l; discharge 15 min).

input voltage, energetic electrons are produced easily, also the formation of active species is accelerated. On the other hand, the change of discharge mode from weak streamer to intense streamers with mixed blue-white light emitted is observable with the increase of input voltage to 46 kV (71 mJ pps). However, the intense spark discharge was produced between two electrodes when input voltage increased to 50 kV (84 mJ pps). The dissolved ozone concentration in water decreased from 0.022 to 0.018 mM during 15 min discharge, exhibiting a higher decrease compared with the case of 46 kV. At the same time, the concentration of hydrogen peroxide also decreased from 0.94 to 0.93 mM. Nevertheless, the decrease of the conversion was very little. This may be due to the fact that high intensity ultraviolet and shockwave were generated during spark discharge and photochemical and cavitation effect were inclined to occur (Locke et al., 2006).

Fig. 4b indicates that the conversion increased with the increase of pulse repetition rate. The energy injected to the reactor increases with the increase of pulse repetition rate, which is beneficial to the conversion. However, the conversion increased very little when pulse repetition rate changes from 100 to 150 pps. This behavior can be explained by the fact that the discharging capacitor, at higher repetition rates, does not have sufficient time to fully re-charge and so the pulse energy decreases (Grabowski, 2006).

### 3.4. Effect of initial solution concentration and volume

The effects of initial solution concentration and volume on the conversion and COD removal are summarized in Fig. 5. Fig. 5a shows that the conversion decreased with the increase of initial solution concentration. Under steady discharge, the active species produced in pulse discharge are maintained at specific concentration levels. The increase of solution concentration leads to the increase of the reaction probability between active species and MO, so the absolute conversion amount increased. The energy yield that corresponds to 40, 60, 80 and 100 mg l<sup>-1</sup> of 0.1 l MO solutions was 2.1, 2.8, 3.4 and 3.6 g (kWh)<sup>-1</sup>,

respectively. When the treating volume was doubled, the conversion only decreased 3%, 4%, 11% and 12%, respectively, compared with the cases of 0.1 l. The height of the solution in pre-oxidation zone increases proportionally with the increase of solution volume, at the same time, the steel mesh barriers fixed in the solution also increase proportionally, leading the journey of ozone in pre-oxidation zone to increase proportionally. The residence time of ozone in pre-oxidation zone is prolonged, thus the dissolved ozone concentration was further increased to 0.04 mM. As a result, even if the treating volume is doubled, the conversion still has no big decrease. The energy yield that corresponds to 40, 60, 80 and 100 mg l<sup>-1</sup> of 0.2 l MO solutions was 4.1, 5.4, 5.9 and 5.9 g (kWh)<sup>-1</sup>, respectively. However, the energy yield has no difference when the solution concentration equals to or exceeds 80 mg l<sup>-1</sup>, implying that the energy yield has reached the maximum value.

The data in Fig. 5b shows that COD removal decreased with the increase of solution concentration and volume. The reactor is so designed that it can utilize ozone produced in pulse discharge. Nevertheless, ozonation may lead to the formation of oxidation byproducts, such as some small molecular acids (Grabowski et al., 2007), which are resistant to ozone attack, and can not be mineralized completely. The pH value decreased from 6.10 to 4.99 and the conductivity increased from 15 to 42  $\mu\text{S cm}^{-1}$  for 0.1 l of 40 mg l<sup>-1</sup> MO solution after electric discharge. Further, the pH value decreased to 4.38 and the conductivity increased to 55  $\mu\text{S cm}^{-1}$  when the solution volume was doubled. The pH and conductivity were not influenced when the solution concentration increased. The concentrations of small molecular acids may become higher with the increase of utilization efficiency of ozone, which may explain the lowering of the solution pH and the increase of the conductivity. Moreover, pulse discharge in air may produce small amount of nitrogen oxides, which may partly diffuse into water and also cause the lowering of the pH (Grabowski et al., 2007). The effect of nitrogen oxides on the chemical reactions was not evaluated in this study.

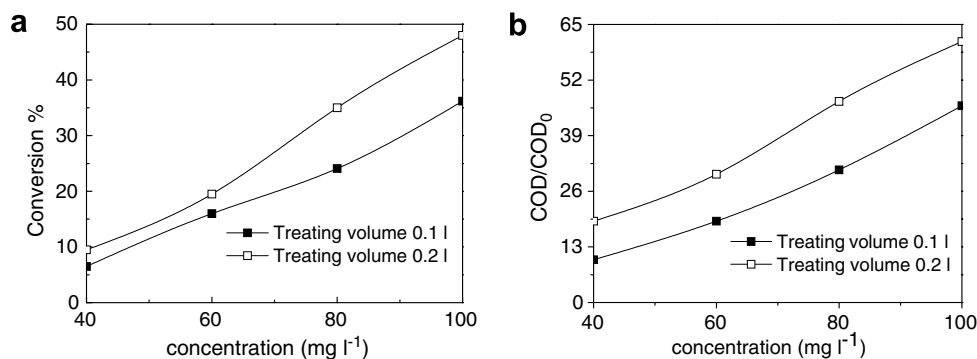


Fig. 5. Effect of initial solution concentration and volume on conversion and COD removal (conditions: five-needle in parallel with needle spacing of 10 mm; needle length in water 4 mm; ground electrode with mesh size of 0.42 mm; electrode gap 17 mm; air flow rate 96 l h<sup>-1</sup>; input voltage 46 kV with 100 pps; discharge 15 min).

#### 4. Conclusions

The present study demonstrates that the novel reactor can be used to efficiently convert MO in aqueous solutions. The concentrations of dissolved ozone and hydrogen peroxide in water increase with the increase of needle numbers. The optimal spacing between neighboring needles also increases with the increase of needle numbers. Electrode gap has an appropriate range, and spark discharge may occur as electrode gap decreases to certain extent and thus may result in the erosion of needle electrodes. Air flow rate presents an economical value at fixed electrode gap. Larger mesh size of ground electrode is favorable for the discharge process. The injection of wastewater above ground electrode for pretreatment and the design of fixed mesh barriers further increase the dissolved ozone concentration in liquid phase. The conversion increases with the increase of input voltage, and higher pulse frequency is advantageous. The conversion decreases while the energy yield increases with the increase of initial solution concentration. The energy yield increases significantly when the treating volume is doubled. COD removal decreases with the increase of solution concentration and treating volume, meanwhile, the solution pH value decreases while the conductivity increases.

#### Acknowledgements

This work is financially supported by National Natural Science Foundation of China (No. 20576079).

#### References

- Bader, H., Hoigne, J., 1981. Determination of ozone in water by the indigo method. *Water Res.* 15, 449–456.
- Chen, J.H., Davidson, J.H., 2002. Electron density and energy distributions in the positive DC corona: interpretation for corona-enhanced chemical reactions. *Plasma Chem. Plasma P.* 22, 199–224.
- Grabowski, L.R., van Veldhuizen, E.M., Pemen, A.J.M., Rutgers, W.R., 2006. Corona above water reactor for systematic study of aqueous phenol degradation. *Plasma Chem. Plasma P.* 26, 3–17.
- Grabowski, L.R., van Veldhuizen, E.M., Pemen, A.J.M., Rutgers, W.R., 2007. Breakdown of methylene blue and methyl orange by pulsed corona discharge. *Plasma Sources Sci. T.* 16, 226–232.
- Grabowski, L.R., 2006. Pulsed Corona in Air for Water Treatment. Ph.D. Thesis, Technische Universiteit Eindhoven, Eindhoven.
- Grymonpré, D.R., Finney, W.C., Clark, R.J., Locke, B.R., 2003. Suspended activated carbon particles and ozone formation in aqueous phase pulsed corona discharge reactors. *Ind. Eng. Chem. Res.* 42, 5117–5134.
- Grymonpré, D.R., Finney, W.C., Clark, R.J., Locke, B.R., 2004. Hybrid gas–liquid electrical discharge reactors for organic compound degradation. *Ind. Eng. Chem. Res.* 43, 1975–1989.
- Hao, X.L., Zhou, M.H., Xin, Q., Lei, L.C., 2007. Pulsed discharge plasma induced Fenton-like reactions for the enhancement of the degradation of 4-chlorophenol in water. *Chemosphere* 66, 2185–2192.
- Kirkpatrick, M.J., Locke, B.R., 2005. Hydrogen, oxygen, and hydrogen peroxide formation in aqueous phase pulsed corona electrical discharge. *Ind. Eng. Chem. Res.* 44, 4243–4248.
- Kim, Y.H., Hong, S.H., 2002. Two-dimensional simulation images of pulsed corona discharges in a wire-plate reactor. In: *IEEE T. Plasma Sci.* 30, 168–169.
- Li, J., Shang, K.F., Wu, Y., Wang, N.H., Zhang, Y., 2007. The experimental research on electrode configuration and discharge characteristics of pulse discharge. *J. Electrostat.* 65, 228–232.
- Locke, B.R., Sato, M., Sunka, P., Hoffmann, M.R., Chang, J.S., 2006. Electrohydraulic discharge and nonthermal plasma for water treatment. *Ind. Eng. Chem. Res.* 45, 882–905.
- Lukes, P., Appleton, A.T., Locke, B.R., 2004. Hydrogen peroxide and ozone formation in hybrid gas–liquid electrical discharge reactors. In: *IEEE T. Ind. Appl.* 40, 60–67.
- Lukes, P., Locke, B.R., 2005. Degradation of substituted phenols in a hybrid gas–liquid electrical discharge reactor. *Ind. Eng. Chem. Res.* 44, 2921–2930.
- Lukes, P., Clupek, M., Babicky, V., Janda, V., Sunka, P., 2005. Generation of ozone by pulsed corona discharge over water surface in hybrid gas–liquid electrical discharge reactor. *J. Phys. D: Appl. Phys.* 38, 409–416.
- Lukes, P., Clupek, M., Babicky, V., Šunka, P., 2006. Erosion of needle electrodes in pulsed corona discharge in water. *Czech. J. Phys.* 56, B916–B924.
- Mok, Y.S., Koh, D.J., Kim, K.T., Nam, I.S., 2003. Nonthermal plasma-enhanced catalytic removal of nitrogen oxides over  $V_2O_5/TiO_2$  and  $Cr_2O_3/TiO_2$ . *Ind. Eng. Chem. Res.* 42, 2960–2967.
- Malik, M.A., ur Rehman, U., Ghaffar, A., Ahmed, K., 2002. Synergistic effect of pulsed corona discharges and ozonation on decolourization of methylene blue in water. *Plasma Sources Sci. T.* 11, 236–240.
- Qu, X.F., Zheng, J.T., Zhang, Y.Z., 2007. Catalytic ozonation of phenolic wastewater with activated carbon fiber in a fluid bed reactor. *J. Colloid Interf. Sci.* 309, 429–434.
- Selles, R.M., 1980. Spectrophotometric determination of hydrogen peroxide using potassium titanium(IV) oxalate. *Analyst* 105, 950–954.
- Vel Leitner, N.K., Syoen, G., Romat, H., Urashima, K., Chang, J.S., 2005. Generation of active entities by the pulsed arc electrohydraulic discharge system and application to removal of atrazine. *Water Res.* 39, 4705–4714.
- Wang, H.J., Jie, L.B., Xie, Q., 2006. Decoloration of azo dye by a multi-needle-to-plate high voltage pulsed corona discharge system in water. *J. Electrostat.* 64, 416–421.
- Yang, B., Zhou, M.H., Lei, L.C., 2005. Synergistic effects of liquid and gas phase discharges using pulsed high voltage for dyes degradation in the presence of oxygen. *Chemosphere* 60, 405–411.
- Yao, S.L., Suzuki, E., Meng, N., Nakayama, A., 2001. Influence of rise time of pulse voltage on the pulsed plasma conversion of methane. *Energy Fuel* 15, 1300–1303.
- Zhang, Y., Zhou, M.H., Hao, X.L., Lei, L.C., 2007. Degradation mechanisms of 4-chlorophenol in a novel gas–liquid hybrid discharge reactor by pulsed high voltage system with oxygen or nitrogen bubbling. *Chemosphere* 67, 702–711.